



Exploring the Antimicrobial Action of Quaternary Amines against *Acinetobacter baumannii*

Gregory A. Knauf,^a Ashley L. Cunningham,^a Misha I. Kazi,^a Ian M. Riddington,^c Alexander A. Crofts,^{a,d} Vincent Cattoir,^{e,f,g} M. Stephen Trent,^d Bryan W. Davies^{a,b}

^aDepartment of Molecular Biosciences, University of Texas at Austin, Austin, Texas, USA

^bCenter for Systems and Synthetic Biology, John Ring LaMontagne Center for Infectious Diseases, Institute for Cellular and Molecular Biology, University of Texas at Austin, Austin, Texas, USA

^cDepartment of Chemistry, University of Texas at Austin, Austin, Texas, USA

^dDepartment of Infectious Diseases, University of Georgia, College of Veterinary Medicine, Athens, Georgia, USA

^eUniversity of Rennes 1, Inserm Unit U1230, Rennes, France

^fDepartment of Clinical Microbiology, University Hospital of Rennes, Rennes, France

^gNational Reference Center for Antimicrobial Resistance (lab 'Enterococci'), Rennes, France

ABSTRACT Quaternary amine compounds (QAC) are potent antimicrobials used to prevent the spread of pathogenic bacteria. While they are known for their membrane-damaging properties, QAC action has been suggested to extend beyond the surface to intracellular targets. Here we characterize the range of action of the QAC biocide benzalkonium chloride (BZK) against the bacterial pathogen *Acinetobacter baumannii*. At high concentrations, BZK acts through membrane disruption, but at low concentrations we show that wide-spread protein aggregation is associated with BZK-induced cell death. Resistance to BZK is found to develop through ribosomal protein mutations that protect *A. baumannii* against BZK-induced protein aggregation. The multifunctional impact of BZK led us to discover that alternative QAC structures, with low human toxicity, retain potent action against multidrug-resistant *A. baumannii*, *Staphylococcus aureus*, and *Clostridium difficile* and present opportunities for their development as antibiotics.

IMPORTANCE Quaternary amine compounds (QACs) are widely used to prevent the spread of bacterial pathogens, but our understanding of their mode of action is incomplete. Here we describe disruption of bacterial proteostasis as an unrecognized action of QAC antimicrobial action and uncover the potential of diverse QAC structures to act as multitarget antibiotics.

KEYWORDS *Acinetobacter baumannii*, BZK, antimicrobial, benzalkonium chloride, biocide, clostridium, proteostasis, quaternary amine

Chemical biocides are commonly used in clinical disinfection to prevent the spread of opportunistic ESKAPE pathogens (*Enterococcus faecium*, *Staphylococcus aureus*, *Klebsiella pneumoniae*, *Acinetobacter baumannii*, *Pseudomonas aeruginosa*, and *Enterobacter* spp.) and *Clostridium difficile* (1–4). Quaternary amine compounds (QACs) are among the most commonly used biocides and are considered nonspecific membrane-active agents (5). The model for their action proposes that their positively charged head group absorbs to acidic components of the bacterial cell envelope and that the long alkyl chains solubilize the membrane, leading to cell death (6, 7). However, several studies indicate that QACs also have intracellular effects that contribute to their antimicrobial action, with the critical lethal action being dependent on the exposure concentration (8–17). The concentrations of QACs recommended for routine use far

Received 26 December 2017 Accepted 10 January 2018 Published 6 February 2018

Citation Knauf GA, Cunningham AL, Kazi MI, Riddington IM, Crofts AA, Cattoir V, Trent MS, Davies BW. 2018. Exploring the antimicrobial action of quaternary amines against *Acinetobacter baumannii*. *mBio* 9:e02394-17. <https://doi.org/10.1128/mBio.02394-17>.

Editor John J. Mekalanos, Harvard Medical School

Copyright © 2018 Knauf et al. This is an open-access article distributed under the terms of the [Creative Commons Attribution 4.0 International license](https://creativecommons.org/licenses/by/4.0/).

Address correspondence to Bryan W. Davies, bwdavies@utexas.edu.

This article is a direct contribution from a Fellow of the American Academy of Microbiology. Solicited external reviewers: Eric Brown, McMaster University; Ian Henderson, University of Birmingham.

exceed that required to eliminate vegetative bacteria under laboratory conditions. But practical conditions, including nonvegetative bacterial growth, the presence of biofilm and nonbiofilm organic matter, high ion concentrations, and pH, can all impact QAC action, allowing bacteria to persist and spread (18–21). Thus, understanding how concentration affects the mechanism of QAC action is critical to understanding and anticipating potential impacts on surviving bacteria.

Here we characterize the action of the commonly used QAC biocide benzalkonium chloride (BZK) against the ESKAPE pathogen *A. baumannii*. While at high concentrations BZK acts primarily through membrane damage, we show that at low concentrations disruption of cellular protein homeostasis (proteostasis) is associated with *A. baumannii* cell death. With this expanded mechanistic understanding, we demonstrate that alternative QAC structures, with low toxicity, still retain their antimicrobial action, opening new scaffolds for design of antibiotics and treatment of multidrug-resistant bacteria.

RESULTS

Cell envelope responses protect *A. baumannii* against BZK. To explore the global effects of BZK exposure on *A. baumannii*, we used transposon insertion mutagenesis with deep sequencing (Tn-seq) and transcriptome sequencing (RNA-seq) to identify genes impacting *A. baumannii* fitness and/or transcriptional responsiveness to sublethal BZK exposure. We used *A. baumannii* strain 17978 for our studies since it has a well-characterized genome (22), is easy to genetically manipulate (23), and showed the median BZK MIC among the nine clinical and laboratory-passaged strains that we tested (see Table S1 in the supplemental material). The sensitivity of our *A. baumannii* strains to BZK was the same using either Mueller-Hinton (MH) broth or lysogeny broth (LB). We used LB for all of the following experiments to maintain a constant growth medium throughout our studies.

For our Tn-seq analysis, we generated and grew an *A. baumannii* 17978 mutant library (~90,000 transposons) in a sublethal BZK dose (5 μ g/ml) to saturation. We anticipated that *A. baumannii* transposon mutants deficient in processes required for BZK resistance would be less fit and would be outcompeted by the remaining population (Fig. 1) (Table S2). In parallel, we used RNA-seq to identify genes induced by the same BZK concentration. We focused on genes that increased in expression with the hypothesis that *A. baumannii* would differentially upregulate cellular functions important for BZK resistance (Fig. 1) (Table S3). We used a cutoff of a ≥ 2 -fold (false-discovery-rate [FDR]-corrected *P* value of < 0.01) decrease in fitness (Tn-seq) or increase in expression (RNA-seq) to broadly capture genes and cellular processes influencing the impact of BZK on *A. baumannii*. This identified 227 genes that promoted *A. baumannii* BZK fitness and 335 genes induced by BZK exposure (Fig. 1) (Table S2 and S3). We analyzed our data sets for gene ontology functional enrichment as previously described (24), but did not identify overrepresented metabolic or cellular processes associated with annotated categories. However, manual inspection identified several genes encoding functions related to four broad categories: cell envelope maintenance, drug efflux, proteostasis, and oxidative stress defense (Fig. 1) (Table S2 and S3).

Cell envelope maintenance functions were prominent in our Tn-seq analysis and included genes encoding outer membrane proteins and enzymes functioning in lipooligosaccharide (LOS) synthesis, phospholipid retrograde maintenance, and peptidoglycan synthesis. This supports the idea of the importance of cell envelope integrity in BZK action. We hypothesized that as a critical target of BZK action, *A. baumannii* may induce expression of genes to bolster or alter cell envelope functions. Interestingly we identified increased expression in only two genes associated with cell envelope functions (*carO*, *wecB*) (Fig. 1) (Table S3). This was intriguing since other cationic membrane-active antimicrobials, such as polymyxins (e.g., polymyxin B, colistin), that bind to and affect the cell surface induce expression of several genes that alter the cell envelope (25). Strain R2, a polymyxin-resistant *A. baumannii* mutant that has an altered LOS charge, was previously isolated (26). We replicated the polymyxin resistance of the R2 strain (see Fig. S1A in the supplemental material), but found that the R2 and parental

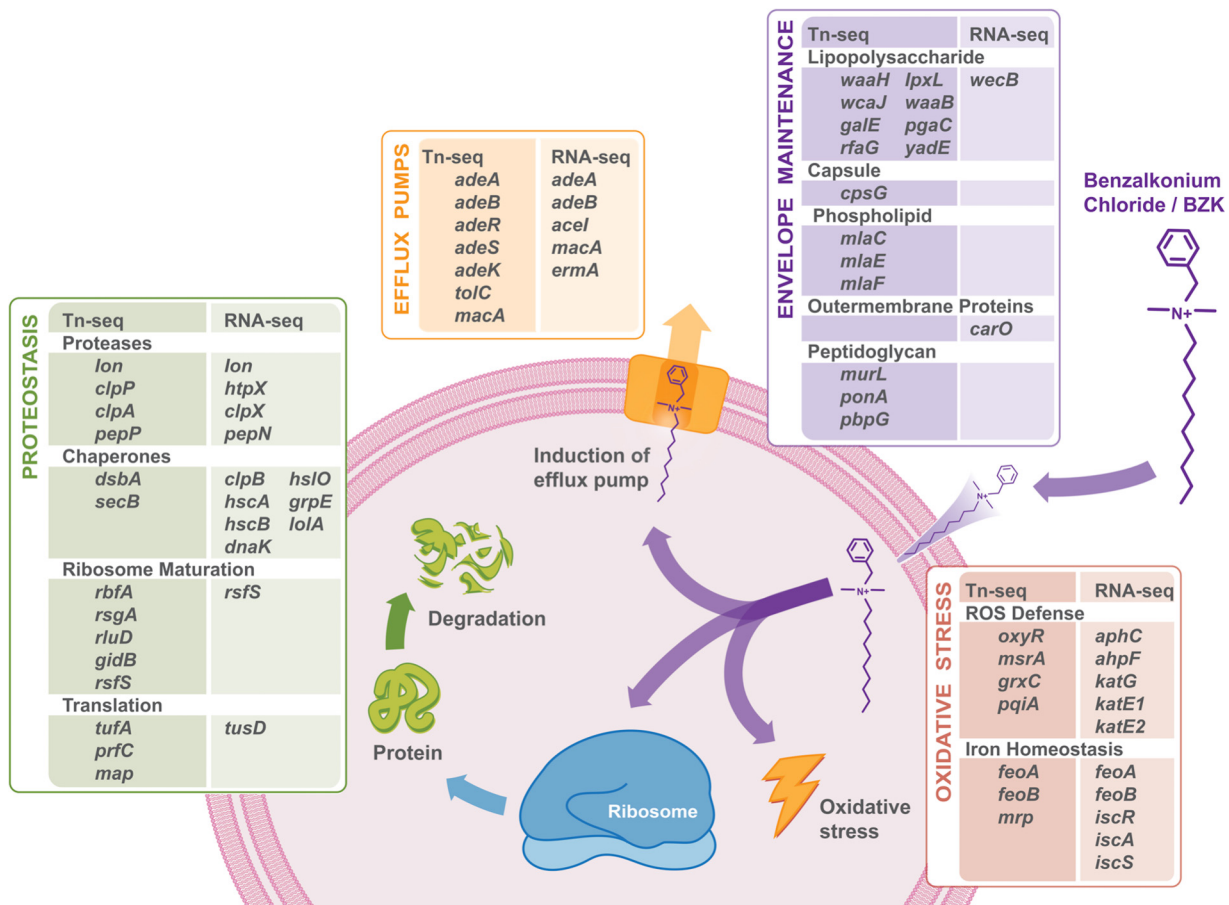


FIG 1 The structure of the C12 form of BZK is shown. Genes identified as promoting *A. baumannii* fitness in BZK (Tn-seq) and upregulated by BZK exposure (RNA-seq) encode functions related to cell envelope maintenance, drug efflux pumps, proteostasis, and oxidative stress defense. Selected genes for each functional group identified in our analysis are shown. ROS, reactive oxygen species.

strains were identical in their sensitivities to BZK (Fig. S1B). This agrees with an earlier study that showed that a *Salmonella enterica* serovar Typhimurium strain with altered surface charge showed no change in BZK sensitivity (27). These results support the idea of the importance of cell envelope integrity for BZK resistance, but indicate that BZK likely interacts with *A. baumannii* membranes differently from cationic-membrane-active agents such as polymyxins.

Drug efflux systems allow bacteria to expel toxic compounds from the cytoplasm, inner membrane, and periplasm (28). We identified *adeA* and *adeB*, which encode subunits of a multidrug efflux system, as strongly induced by BZK and important for *A. baumannii* fitness (Fig. 1). Insertions in *adeA* and *adeB* or in *adeR* and *adeS*, encoding the two-component regulatory system, decreased *A. baumannii* fitness during BZK exposure (Table S2). BZK induced *adeAB* expression as measured by RNA-seq (Table S3). An *A. baumannii* 17978 Δ *adeB* strain showed a 5-log decrease in colony formation on agar containing BZK compared to the wild-type strain, supporting the idea of the importance of this efflux pump in *A. baumannii* defense against BZK (Fig. S2). AdeA and AdeB commonly function with a third component, AdeC, to form the AdeABC tripartite drug efflux system. *A. baumannii* 17978 does not encode AdeC, but does encode a homolog, AdeK, which was identified as affecting *A. baumannii* fitness in our Tn-seq analysis and which may function with AdeA and AdeB. Our results support data from previous studies linking AdeABC to BZK and broader biocide susceptibility in *A. baumannii* (29–31) and suggest an action for BZK past the outer membrane.

Intracellular responses protect *A. baumannii* against BZK. Since BZK action is attributed to cell envelope disruption, we were intrigued that transposon insertions

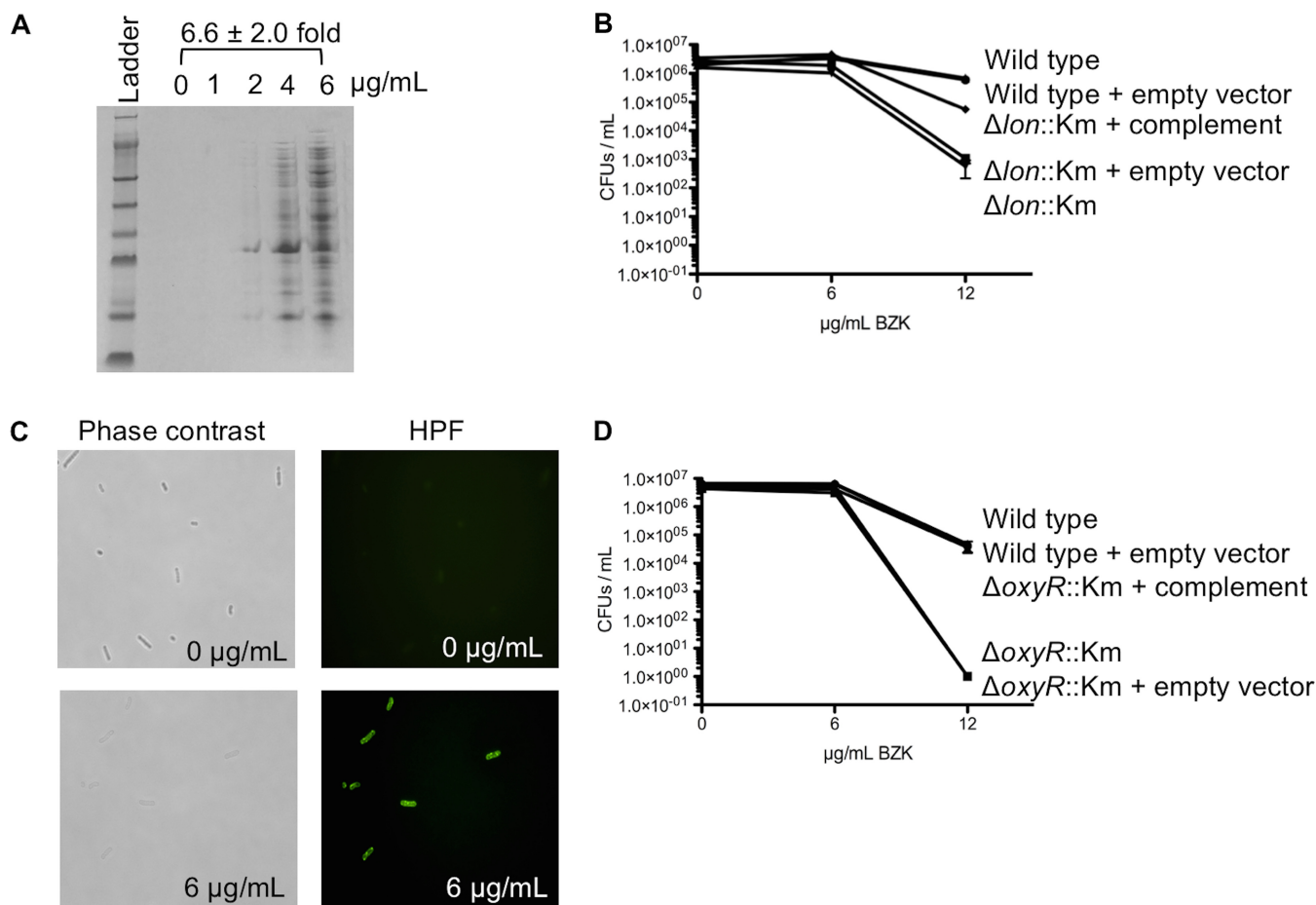


FIG 2 BZK impacts proteostasis and oxidative stress response. (A) Protein aggregates from *A. baumannii* wild type (WT) treated with increasing levels of BZK. The amount of aggregate loaded from each sample was normalized by cell number. The experiment was repeated at least three times, with a representative result shown. Treatment with 6 $\mu\text{g}/\text{mL}$ BZK resulted in a 6.6-fold \pm 2.0-fold increase in aggregates compared to no treatment; $P < 0.05$ (unpaired two-tailed Student's *t* test). (B) Plating efficiency of *A. baumannii* wild-type strain and Δlon mutant on increasing concentrations of BZK agar. At 12 $\mu\text{g}/\text{mL}$, the wild-type strain showed higher plating efficiency than the mutant; $P < 0.05$ (unpaired two-tailed Student's *t* test). At 12 $\mu\text{g}/\text{mL}$, the combination of the wild-type strain with vector (Wild type + empty vector) showed higher plating efficiency than the mutant + vector and the complemented strain; $P < 0.05$ (one-way analysis of variance [ANOVA], Tukey posttest). (C) Phase-contrast and HPF fluorescence microscopy images of wild-type *A. baumannii* with and without 6 $\mu\text{g}/\text{mL}$ sub-MIC BZK treatment. (D) Plating efficiency of *A. baumannii* wild-type strain and $\Delta oxyR$ mutant on increasing concentrations of BZK agar. At 12 $\mu\text{g}/\text{mL}$, the wild-type strain showed higher plating efficiency than the mutant; $P < 0.05$ (unpaired two-tailed Student's *t* test). At 12 $\mu\text{g}/\text{mL}$, the wild-type strain + vector showed higher plating efficiency than the mutant + vector, but not than the complemented strain; $P < 0.05$ (one-way ANOVA, Tukey posttest).

disrupting intracellular proteostasis and oxidative defense affected BZK fitness as strongly as many envelope maintenance functions in our Tn-seq analysis (Fig. 1) (Table S2). Insertions in genes encoding products associated with ribosome biogenesis (RsgA, RluD, RimL), translation control (PrfC, Map), and damaged/aggregated protein turnover (Lon, ClpP) decreased *A. baumannii* BZK fitness (Table S2). Correlatively, BZK induced expression of several genes encoding products associated with damaged/aggregated protein turnover and protein folding functions (Lon, HtpX, ClpB, HscB) (Table S3). Similar proteostasis gene expression responses have been observed in bacteria following treatment with ribosomal antibiotics and have been linked to protein damage, with formation of deleterious protein aggregates (32–35). We assayed the impact of sublethal BZK on the proteome of *A. baumannii* and observed a dose-dependent increase in total protein aggregate levels (Fig. 2A), indicating that BZK was disrupting proteostasis. We assayed the ability of the membrane-disrupting cationic antibiotic colistin to induce protein aggregates. Treatment of *A. baumannii* with an equivalent sublethal dose of colistin did not induce protein aggregates (Fig. S3A), indicating that the membrane disruption alone was likely not inducing the observed aggregate formation. Many proteins share overlapping functions in the prevention and

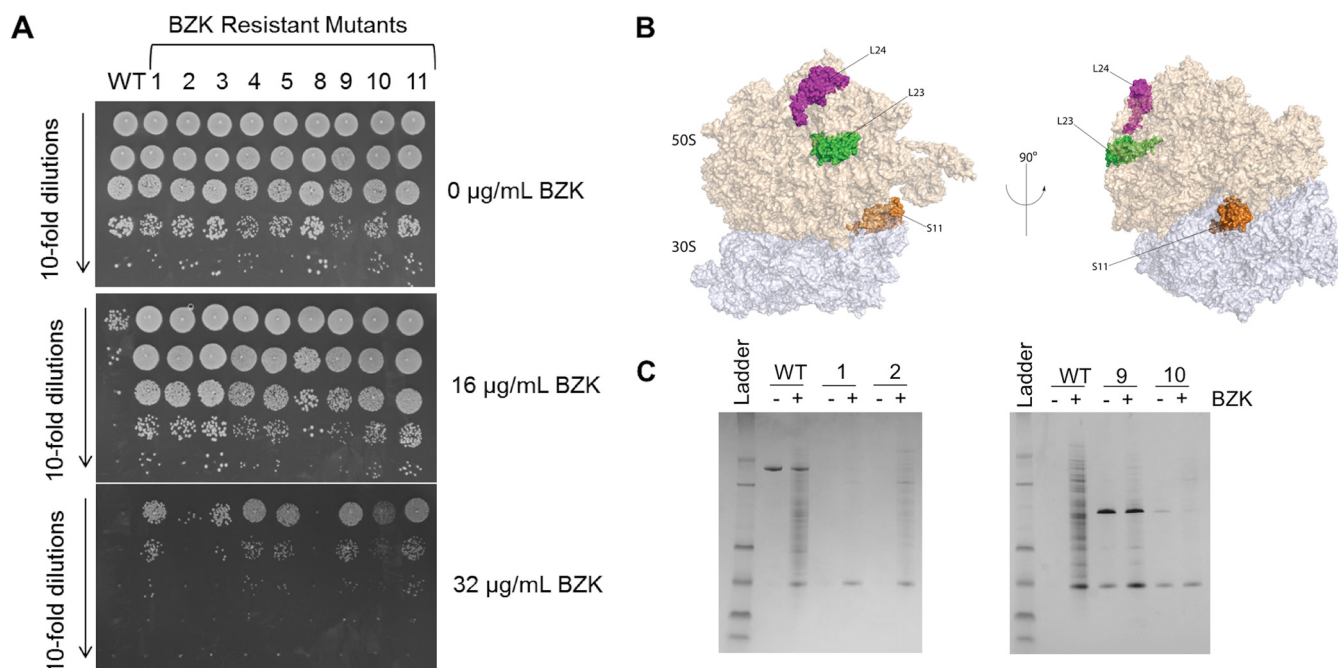


FIG 3 BZK-resistant mutant phenotypes and ribosome locations. (A) Plating efficiency of *A. baumannii* 17978 (WT) and BZK-resistant mutants on 0, 16, and 32 µg/ml BZK plates. (B) Ribosomes showing locations of proteins with mutations affecting BZK sensitivity. (C) Protein aggregates from *A. baumannii* 17978 (WT) and BZK-resistant mutants 1, 2, 9, and 10 with (+) or without (-) 6 µg/ml sub-MIC BZK treatment. The amount of aggregate loaded from each sample was normalized by cell number.

the turnover of protein aggregates, diminishing the effect of loss of any one proteostasis factor (36, 37). Nevertheless, we did find that deletion of Lon protease alone was sufficient to decrease the ability of *A. baumannii* to form colonies on agar containing BZK, further linking effects on proteostasis with BZK action (Fig. 2B). Correlatively, more protein aggregates accumulated in the Δlon strain than in the wild type following BZK exposure (Fig. S3B and C).

Tn-seq indicated that the master oxidative stress regulator OxyR contributed to BZK resistance (Fig. 1) (Table S2), and expression levels of OxyR-regulated genes, including all genes encoding catalases (*kat*) and alkyl hydroperoxidases (*ahp*), were induced following BZK exposure (Fig. 1) (Table S3). We visualized BZK-induced oxidative stress using the redox-sensitive fluorescent dye hydroxyphenyl fluorescein (HPF), which accumulates in the cell and fluoresces upon oxidation. Exposure of *A. baumannii* to sublethal BZK levels, and treatment with HPF, resulted in highly fluorescent cells (Fig. 2C), supporting the idea of an induction of oxidative stress by BZK. Furthermore, deletion of *oxyR* decreased the ability of *A. baumannii* to form colonies on BZK agar, supporting the idea of a role for oxidative stress in BZK-induced lethality (Fig. 2D).

Ribosomal protein mutations promote BZK resistance. Our results indicate that BZK can act through disruption of intracellular processes, but the potential target(s) remained unclear. Target mutation is a common mechanism by which drug resistance is acquired. To leverage this unbiased approach, we performed a single-passage selection for spontaneous *A. baumannii* mutants that could grow on agar containing twice the concentration of BZK that the parental strain can tolerate. After a single passage, we isolated 11 *A. baumannii* mutants whose agar MIC had increased from 16 µg/ml to 32 µg/ml. This corresponds to a 100× to 1,000× increase in CFU survival when spotted on BZK-containing medium (Fig. 3A). We sequenced the genomes of these 11 BZK-resistant mutants and compared them to the resequenced parental genome to identify potential mutations. We identified unique mutations in 9 of the 11 BZK resistant strains, each confirmed by Sanger sequencing. Remarkably, 8 of 9 isolates carried mutations in ribosomal proteins or the untranslated region (UTR) between two ribosomal protein

TABLE 1 Mutation locations of BZK-resistant *A. baumannii* mutants

Strain	BZK MIC ($\mu\text{g/ml}$) ^a	Protein/feature-encoding mutation	Amino acid change
Parental	16		
Mutant 1	32	Ribosome protein operon UTR	None
Mutant 2	32	L23	I42F
Mutant 3	32	L24	Frameshift
Mutant 10	32	L24	G15V
Mutant 11	32	L24	I4N
Mutant 9	32	S11	D111Y
Mutant 4 ^b	32	S11	A62D
Mutant 5 ^b	32	S11	A62D
Mutant 4 ^b	32	SecY	L306I
Mutant 5 ^b	32	SecY	L306I
Mutant 8	32	Hypothetical (A1S_1648)	S137F

^aData represent MIC values determined by the agar microdilution method.

^bThe identical two mutations were identified in these isolates.

operons (Table 1). Among the 9 mutants, 7 had a single mutation. Mutants 3, 10, and 11 each had a unique mutation in the 50S protein L24. The mutation in isolate 1 was found in the UTR between two ribosomal protein operons. The mutations in isolates 2 and 9 were found in L23 and S11, respectively. Mutants 4 and 5 appeared to be siblings as they shared two identical mutations in S11 and SecY. Ribosomal proteins L23 and L24 are located together near the exit tunnel and interact with SecY during protein secretion (38), while S11 is a component of the ribosomal P site and interacts with S7 to influence translation fidelity (39) (Fig. 3B). Mutant 8 carried a single mutation in a gene coding for a hypothetical protein of unknown function.

BZK-resistant mutants protect against protein aggregation. Our omic results, combined with our observation of BZK-induced protein aggregation and of BZK resistance resulting from ribosomal protein mutations, suggested that part of the antimicrobial action of BZK may occur through disruption of proteostasis. However, ribosome mutations can have pleiotropic effects, including affecting bacterial growth rate, which can influence drug action. We tested the BZK-resistant mutants and found they all had growth rates similar to that of the parental strain, suggesting that their BZK resistance was not due to growth effects (Fig. S4). We also considered that BZK-resistant mutants might indirectly strengthen cell membranes against BZK. We assayed the membrane permeability of these mutants by measuring propidium iodide (PI) uptake. However, we found no significant difference in the levels of PI uptake between the parental and mutant strains following BZK treatment (Fig. S5A).

A study in *Mycobacterium smegmatis* indicated that ribosomal protein mutations could promote resistance to several classes of antibiotics (40). We determined the activity of antibiotics targeting different cellular pathways against the BZK-resistant mutants (Table 2). The levels of sensitivity to the membrane-damaging antibiotic polymyxin B did not differ between the parental and mutant strains (Table 2), further indicating they do not have altered cell membranes. Mutants with mutations affecting L23 and L24 and the UTR upstream of the L24 operon showed increased resistance to erythromycin, but not to other ribosomal antibiotics. Different subsets of BZK-resistant mutants conferred resistance to rifampin, ciprofloxacin, and carbenicillin, while other subsets conferred increased sensitivity to telithromycin and gentamicin (Table 2).

While it is unclear how ribosomal mutations influence the activity of these various antibiotics, we hypothesized that the ribosomal protein mutations may confer resistance to BZK by stabilizing the *A. baumannii* proteome. We treated mutants 1, 2, 9, and 10, representing distinct ribosome protein mutations, with BZK and analyzed their protein aggregate profiles. All four BZK-resistant mutants showed reduced protein aggregate formation compared to the parental strain (Fig. 3C). The correlation of reduced protein aggregation and BZK resistance further suggests that BZK may act in part through disruption of intracellular proteostasis.

TABLE 2 Antibiotic sensitivity of BZK-resistant *A. baumannii* mutants

Strain	Mutation site(s)	MIC ($\mu\text{g/ml}$) ^a									
		BZK	Pxb	Erm	Tem	Clm	Gem	Tet	CIP	Rif	Cbn
Parental		16	1	8	8	64	8	1	0.25	2	32
Mutant 1	UTR	32	1	16	8	64	8	1	1	4	32
Mutant 2	L23	32	1	16	8	64	8	1	0.5	4	32
Mutant 3	L24	32	1	16	8	64	8	1	0.5	4	32
Mutant 4 ^b	S11, SecY	32	1	8	8	64	4	1	0.5	4	64
Mutant 5 ^b	S11, SecY	32	1	8	8	64	4	1	0.5	4	64
Mutant 8	A15_1648	32	1	8	8	64	8	1	0.25	2	32
Mutant 9	S11	32	1	8	4	64	8	1	0.5	2	32
Mutant 10	L24	32	1	8	8	64	4	1	1	4	64
Mutant 11	L24	32	1	16	8	64	8	1	1	4	32

^aData represent MIC values determined by the agar microdilution method. BZK, benzalkonium chloride; Cbn, carbenicillin; Cip, ciprofloxacin; Clm, clindamycin; Erm, erythromycin; Gem, gentamicin; Pxb, polymyxin B; Rif, rifampin; Tem, telithromycin; Tet, tetracycline.

^bThe identical two mutations were identified in these isolates.

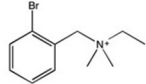
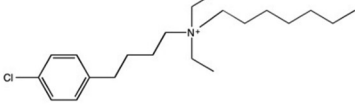
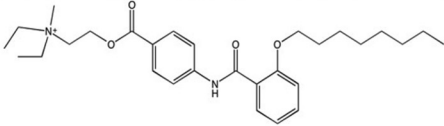
We hypothesize that BZK may directly inhibit protein translation. We measured the effect of BZK on the translation of a known protein (dihydrofolate reductase [DHFR]) with an *in vitro* *Escherichia coli* transcription-translation system. Addition of erythromycin to the *in vitro* reaction effectively inhibited translation of DHFR; however, BZK did not have an effect on *in vitro* DHFR translational activity (Fig. S5B).

The known effects of BZK on membrane integrity and the resistance mutations seen in secretion-related proteins such as SecY, L23, and L24 (Table 1) led us to question whether BZK might affect some classes of proteins more than others. We analyzed the protein content of aggregates in *A. baumannii* with and without sub-MIC BZK treatment by mass spectroscopy (Table S4). While the treated sample produced significantly more total aggregates, the two samples shared the majority of identified proteins, 1,388 proteins, in common. Only three proteins were unique to the untreated sample and seven to the treated sample. We also did not identify any major enrichment of specific cellular classes of proteins using Gene Ontology (GO) terms (Table S4). This result suggests that the effects of BZK on proteostasis are not specific to any one class of protein.

Therapeutic QACs have antimicrobial action. QAC biocides were developed for their membrane action and favor long alkyl tails, which also promote cytotoxicity and exclude their use as antibiotics (13). However, our results implicating additional processes in BZK action led us to ask if QACs with less-toxic structures could still retain antimicrobial activity. We identified three candidates (Table 3); bretylium tosylate and clofilium tosylate are antiarrhythmic agents, while otilonium bromide (OB) is a muscarinic receptor inhibitor used to treat irritable bowel syndrome (IBS) (41–43). We tested each QAC against *A. baumannii* 17978 and multidrug-resistant (MDR) *A. baumannii* AYE. Since QACs are frequently more effective against Gram-positive bacteria (6), we also tested *Staphylococcus aureus* and *Clostridium difficile*. Due to the instability of otilonium bromide (44), we measured the activity of these compounds by a minimal bactericidal concentration (MBC) assay (45) (Table 3). Bretylium tosylate showed no effect against any strain. Clofilium tosylate showed activity against *A. baumannii* strains and a more potent effect against *S. aureus* strains. Remarkably, otilonium bromide exhibited potent activity against all bacteria and was slightly more effective against *C. difficile* strain 630 than the antibiotic vancomycin (Table 3), which is often used for the treatment of severe *C. difficile* infections (46).

Otilonium bromide is structurally distinct from BZK. To determine if otilonium bromide acted similarly to BZK, we assayed its impact on membrane permeability and protein aggregation. We assayed membrane permeability by measuring uptake of PI following a sublethal treatment with otilonium bromide. Otilonium bromide increased the population fluorescence in *A. baumannii* and *S. aureus* in a dose-dependent manner, indicating that it was capable of inducing membrane permeability (Fig. 4A). Otilonium bromide also

TABLE 3 Minimal bactericidal concentration assay of clinically used and explored QACs and vancomycin

Compound	<i>A. baumannii</i>		<i>S. aureus</i>		<i>C. difficile</i>	
	17978	AYE	Newman	MU50	43255	630
	>256	>256	>256	>256	>256	>256
Bertylium tosylate (µg/ml)	>256	>256	>256	>256	>256	>256
	128	128	32	64	nd	nd
Clofilium tosylate (µg/ml)	128	128	32	64	nd	nd
	16	16	8	8	1	2
Otilonium bromide (µg/ml)	16	16	8	8	1	2
Vancomycin (µg/ml)	nd	nd	1	2	1	4
nd – not determined						

induced accumulation of protein aggregates in both *A. baumannii* and *S. aureus* following a sublethal exposure (Fig. 4B). Our results indicate that both membrane actions and proteostasis actions are conserved in antimicrobial QACs and that nontoxic QAC scaffolds represent potent leads for antibiotic development.

DISCUSSION

QACs have been staple biocides since the 1930s (47). While QAC disruption of cell membranes is well established, its effects at low concentrations have remained unclear. Our results suggest that disruption of proteostasis is an important pathway of BZK antimicrobial action at low concentrations. Quaternary amines are excellent phase

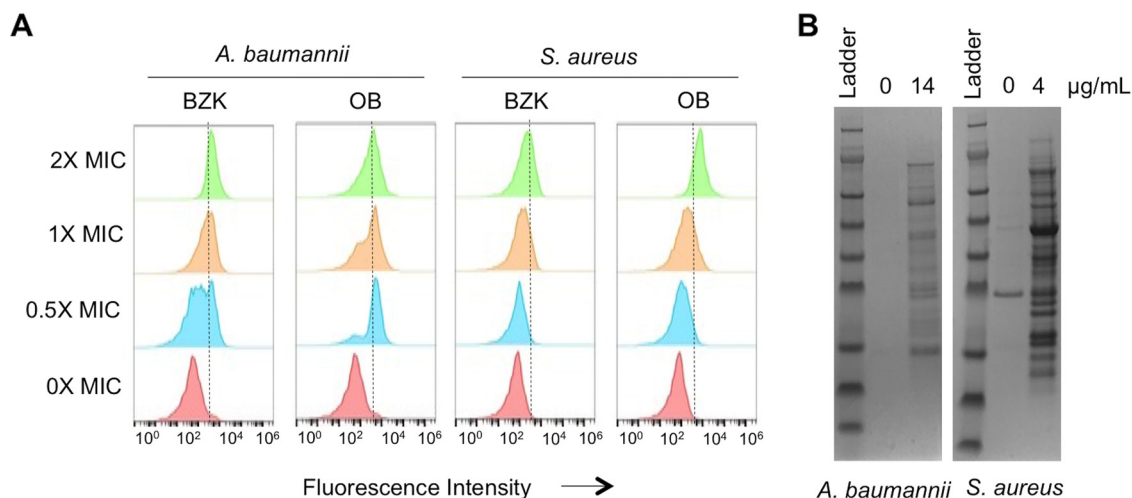


FIG 4 BZK and OB have similar cellular effects. (A) Membrane damage caused by BZK and OB at 0× to 2× MIC in *A. baumannii* and *S. aureus* measured by cell uptake of propidium iodide. Increased fluorescent intensity indicates increased propidium iodide uptake and membrane damage. Equal numbers of cells were counted under all conditions. (B) Subinhibitory OB treatment induces aggregate formation in *S. aureus* and *A. baumannii*. The amount of aggregate loaded from each sample was normalized by cell number as described in the Fig. 2 legend.

transfer catalysts, being soluble in both aqueous and organic solvents (48). In this context, the alkyl chain of BZK could mediate transition of the quaternary amine through hydrophobic cell membrane barriers to affect cytosolic factors controlling proteome homeostasis. The positively charged quaternary amine may interact with many negatively charged intracellular molecules such as RNA and DNA. During this transition, efflux pumps can be activated, which eliminates BZK from the cell. Our studies specifically implicate the AdeABC efflux system in *A. baumannii* BZK resistance. Expression of the AdeABC efflux pump has been linked to broad-spectrum antibiotic resistance in *Acinetobacter* spp. (30, 31). BZK-induced or BZK-selected upregulation of *adeABC* could support antibiotic cross-resistance. Our results demonstrate that BZK can select for ribosomal mutations that confer cross-resistance to different classes of antibiotics. This impact of ribosomal protein mutation was also observed for *M. smegmatis* (40). The potential for QAC-antibiotic cross-resistance has been reported in several studies (7); however, a consensus on its importance to public health has not been reached (49). Our discovery of BZK as a driver for ribosomal mutations that promote broad antibiotic resistance may help provide a focus on the public health impact of QAC-ribosomal antibiotic cross-resistance.

Our omic results, combined with our observation of BZK-induced protein aggregation and BZK resistance mediated by ribosomal protein mutations, suggest that part of the BZK antimicrobial action occurs through disruption of cellular proteostasis. How BZK elicits this effect is unclear. Our results indicated that BZK does not directly inhibit protein translation *in vitro*. While it is still possible that BZK directly acts on the ribosome *in vivo*, it may also influence ribosome association with other important proteostasis components. The single amino acid substitution L23 and L24 mutations may promote chaperone interactions to protect nascent polypeptides at the exit tunnel to prevent their aggregation. The chaperone Trigger Factor docks on L23 to interact with nascent peptides and protect them during maturation (50). Cryo-electron microscopy showed that L23 and L24 directly interact with SecY and nascent polypeptides (38). The mutations in L23, L24, and SecY conferring BZK resistance may alter the interactions of this complex to better chaperone proteins for export. While we did not identify a bias in proteins found in aggregate with and without BZK treatment, it is possible that the presence of an increased amount of specific proteins has a strong impact on BZK tolerance.

We also identified mutations in the small 30S subunit affecting S11. A previous study also reported a mutation in the S1 30S protein in an *E. coli* strain with increased BZK resistance (15). These mutations may have long-range effects or could implicate more than one ribosomal target in BZK action. Mutant 1 has a solitary mutation in a ribosomal protein operon untranslated region. This mutation potentially could interfere with transcription termination of the upstream operon. The result would be increased transcription from readthrough, potentially causing upregulation of the downstream ribosomal proteins, including L24. L24 is an initiator of 50S subunit assembly (51) which, if overexpressed, could potentially have important effects on 50S subunit assembly. The possibility of a similar type of effect on assembly cannot be excluded for mutants 3, 10, and 11, which have mutations in L24. Protection against protein aggregation also provides a rationale for the associated impact of oxidative stress on BZK survival. Damage to protein during synthesis has been proposed to disrupt membrane integrity and trigger increased production of reactive oxygen species (32). Damaged and unfolded proteins are in turn more susceptible to oxidative damage that can further amplify the proteome damage (33). However, the dramatic effect of otilonium bromide on *C. difficile*, which is grown anaerobically, indicates that the effects of oxidative stress are likely not as critical as the impact on protein quality control. Future studies to clarify BZK proteostasis effects and how ribosomal protein mutations facilitate BZK resistance will provide sharper insight into the full spectrum of BZK action.

Regardless of the details of the mechanism, our observation of the impact of BZK beyond the cell envelope led us to explore QACs with structures not typically associated with antimicrobial action. Our results highlight the possibility of using QACs as

scaffolds for antibiotic development. Otilonium bromide shows potent activity against multidrug-resistant *A. baumannii*, *S. aureus*, and *C. difficile* and is safe for oral human use (42). It shows low toxicity through several routes of delivery (52, 53). At therapeutic doses, the concentration of otilonium bromide in the intestine and colonic smooth muscle reaches approximately 5 to 6 $\mu\text{g/ml}$, which is $2\times$ to $3\times$ higher than the MBC that we determined for *C. difficile*. The C8 alkyl tail is shorter than those typically associated with QAC activity (6), but is similar in length to the C9 tail of daptomycin. Otilonium bromide is an antimuscarinic used to treat IBS that acts by inhibiting muscarinic receptor-coupled calcium signaling (42). Advances in microbiome research have revealed important connections between our gut flora and IBS (54). Thus, in addition to its antimuscarinic activity, otilonium bromide may also alleviate IBS symptoms by eliminating antagonistic microbes. Our identification of an intracellular action for BZK shows similarities to the findings described for the biocide Tricolsan. Like BZK, triclosan disrupts cell membranes, but it was also shown to specifically inhibit the FabI enzyme (55). This finding has spurred pursuit of FabI inhibitors as antibiotics (56).

MATERIALS AND METHODS

Bacterial strains and plasmids used. All bacterial strains and plasmids used, along with their sources, are described in Table S5 in the supplemental material.

Growth conditions and genetic manipulations. Bacteria were cultured in lysogeny broth (LB) broth at 37°C unless otherwise stated. *Clostridium difficile* was grown with brain heart infusion medium with yeast extract (BHIS) and reinforced clostridial medium (RCM). Carbenicillin (75 $\mu\text{g/ml}$), kanamycin (25 $\mu\text{g/ml}$), gentamicin (10 $\mu\text{g/ml}$), chloramphenicol (10 $\mu\text{g/ml}$), and tetracycline (10 $\mu\text{g/ml}$) were used for selection. Benzalkonium chloride was from Sigma and was a mixture of the C12 and C14 alkyl chain lengths. Clofilium tosylate and otilonium bromide (OB) were purchased from Sigma. Gene deletion and complementation were conducted as previously described (23).

MICs, minimal bactericidal concentrations, and plating efficiency assay. Agar dilution method MICs were determined using standard procedures in LB, BHIS, or RCM (57). All media containing quaternary amines or antibiotics were prepared on the day of use. Minimal bactericidal concentrations (MBC) to determine 99.9% viability reduction were conducted using standard procedures (45). For CFU assays, overnight cultures were diluted to approximately 10^6 to 10^7 CFU/ml. Each culture was serially diluted and plated onto agar plates with or without increasing concentrations of BZK. CFU counting was performed after overnight growth. All assays were performed in at least biological triplicate.

Tn-seq and RNA-seq. For Tn-seq analysis, an *A. baumannii* mutant transposon library (~90,000 transposons) for sequencing was constructed as previously described (58) using gentamicin and chloramphenicol to select for transconjugants. Library aliquots were diluted to $\sim 10^7$ CFU/ml in 5 ml of LB medium with or without 5 $\mu\text{g/ml}$ BZK and grown to saturation at 25°C with shaking. Bacteria were pelleted and processed for transposon sequencing as previously described (58). For RNA-seq, fresh *A. baumannii* colonies were collected from LB plates and diluted to $\sim 10^8$ CFU/ml in 5 ml of LB growth medium. Cultures were grown and treated with or without 5 $\mu\text{g/ml}$ BZK for 45 min at 25°C with shaking. The cells were pelleted and processed for RNA sequencing as previously described (59). Both RNA-seq and Tn-seq data were aligned to the *A. baumannii* 17978 genome and analyzed using CLC Genomics Workbench software and reads per kilobase per million (RPKM) values. The statistical test performed was a Baggerley's test of the proportions of counts in each group of samples to generate a *P* value associated with the weighted proportions of fold change between the experiment and control groups for each gene. We used an arbitrary cutoff of 2-fold weighted proportion change with an FDR-corrected *P* of <0.01. Nonessential genes were identified for Tn-seq analysis based on previous results (60).

BZK-resistant mutant isolation. Two milliliters of a saturated *A. baumannii* culture ($\sim 10^{10}$ /ml) was pelleted and suspended in 200 μl of LB. The 200- μl suspension was spread on LB agar containing 32 $\mu\text{g/ml}$ BZK. The plates were incubated overnight at 37°C. After incubation, single colonies were picked and streaked on 16 $\mu\text{g/ml}$ benzalkonium chloride LB plates. These plates were then incubated overnight and analyzed to confirm increased resistance to BZK. Samples that successfully grew on 16 $\mu\text{g/ml}$ BZK after streaking had their MICs for BZK and antibiotics determined by the agar dilution method.

Genomic variant analysis. Single-nucleotide polymorphisms were identified as described previously (24). Briefly, extracted genomic DNA was processed for Illumina HiSeq sequencing using an NEB Next Ultra DNA Library Prep Kit. Genome sequences were aligned and single-nucleotide polymorphisms detected using CLC Genomic Workbench software. Variants were called with over 50-fold coverage at a frequency of 70%. False positives were manually checked for and removed from the results. All mutations were validated by Sanger sequencing.

Fluorescence microscopy. Exponentially growing *A. baumannii* cultures were normalized to an optical density at 600 nm (OD_{600}) of ~ 0.4 and treated with 0 or 6 $\mu\text{g/ml}$ BZK for 30 min with shaking at 37°C. One milliliter of each sample was pelleted and resuspended in $1\times$ phosphate-buffered saline (PBS) with 5 μM 3'-(p-hydroxyphenyl)fluorescein (Thermo Fisher H36004). The suspensions were incubated in the dark for 15 min and then resuspended in 1 ml of fresh PBS. Ten microliters of the cell suspension was then allocated onto a slide and imaged.

Protein aggregate isolation. Cellular protein aggregate isolation and analysis were performed as previously described (37). Briefly, 50-ml LB cultures of exponentially growing bacteria were treated with the indicated concentration of BZK or otilonium bromide. Following isolation, aggregates were normalized and separated by SDS-PAGE and Coomassie stained for visualization. Aggregates were quantified using the area density feature in VisionWorks LS software (UVP, Inc.) on an image of the aggregate gel.

Aggregate proteomics. Protein identification was provided by the Proteomics Facility at the University of Texas at Austin following previously published procedures (61). Scaffold (version Scaffold_4.8.2; Proteome Software Inc., Portland, OR) was used to validate tandem mass spectrometry (MS/MS)-based peptide and protein identifications. Tandem and Sequest were set up to search *acinetobacter_07-15.fasta* (unknown version; 3,798 entries), assuming the presence of the digestion enzyme trypsin. Peptide identifications were accepted if they could be established at greater than 89.0% probability to achieve an FDR of less than 1.0%. Peptide probabilities evaluated using Sequest software were assigned by the Scaffold Local FDR algorithm. Peptide probabilities evaluated using X! Tandem software were assigned by the Peptide Prophet algorithm (62) with Scaffold delta-mass correction. Protein identifications were accepted if they could be established to achieve an FDR of less than 5.0% at greater than 99.0% probability and contained at least 2 identified peptides. Protein probabilities were assigned by the Protein Prophet algorithm (63). Proteins that contained similar peptides and that could not be differentiated based on MS/MS analysis alone were grouped to satisfy the principles of parsimony. Proteins were annotated with Gene Ontology (GO) terms from *gene_association.goa_uniprot* (downloaded 14 January 2015) (64). Relative abundances were quantified by the use of normalized exponentially modified protein abundance index (emPAI) values, with a minimal value setting of 0.

Flow cytometry. Bacterial cell membrane damage and pore formation induced by BZK and OB were examined by detection of propidium iodide (PI) influx (66). The bacteria were cultured at 37°C to mid-log phase and then diluted to an OD₆₀₀ of 0.1 in PBS. BZK and OB were added to a 500- μ l bacterial suspension at concentrations of 0 \times to 2 \times MIC and incubated for 30 min. Bacteria were collected and resuspended in buffer. PI solution was added to reach a final concentration of 2 μ g/ml. The fluorescence signal in treated cells was determined by flow cytometry (BD Accuri) and further analyzed with FlowJo (Treestar, USA).

In vitro translation assay. *In vitro* translation was performed with an NEB PURExpress *in vitro* protein synthesis kit per the protocol described by the manufacturer. S35-methionine was used to measure production of the model protein DHFR.

Data availability. Tn-seq and RNA-seq data have been deposited with the NCBI's Gene Expression Omnibus under GenBank accession number [GSE96913](https://www.ncbi.nlm.nih.gov/geo/query/acc.cgi?acc=GSE96913). Whole-genome sequencing data were deposited with NCBI's Sequence Read Archive under accession numbers [SRR5343897](https://www.ncbi.nlm.nih.gov/sra/acc.cgi?acc=SRR5343897) to [SRR5343908](https://www.ncbi.nlm.nih.gov/sra/acc.cgi?acc=SRR5343908).

SUPPLEMENTAL MATERIAL

Supplemental material for this article may be found at <https://doi.org/10.1128/mBio.02394-17>.

FIG S1, PDF file, 1.2 MB.

FIG S2, PDF file, 0.3 MB.

FIG S3, PDF file, 0.8 MB.

FIG S4, PDF file, 0.5 MB.

FIG S5, PDF file, 0.5 MB.

TABLE S1, PDF file, 0.02 MB.

TABLE S2, PDF file, 0.5 MB.

TABLE S3, PDF file, 0.7 MB.

TABLE S4, PDF file, 1.4 MB.

TABLE S5, PDF file, 0.02 MB.

ACKNOWLEDGMENTS

B.W.D., G.A.K., I.M.R., V.C., and M.S.T. designed the experiments. B.W.D., G.A.K., A.L.C., M.I.K., I.M.R., and A.A.C. performed the experiments. B.W.D. and G.A.K. wrote the manuscript.

B.W.D. was supported by NIH grant AI-125337, Army Research Office grant W911NF-16-1-0146, and Welch Foundation grant F-1870. M.S.T. was supported by NIH grants AI064184 and AI076322 and by Army Research Office grant W911NF-12-0390.

REFERENCES

1. Abreu AC, Tavares RR, Borges A, Mergulhão F, Simões M. 2013. Current and emergent strategies for disinfection of hospital environments. *J Antimicrob Chemother* 68:2718–2732. <https://doi.org/10.1093/jac/dkt281>.
2. Boucher HW, Talbot GH, Bradley JS, Edwards JE, Gilbert D, Rice LB, Scheld M, Spellberg B, Bartlett J. 2009. Bad bugs, no drugs: no ESCAPE! An update from the Infectious Diseases Society of America. *Clin Infect Dis* 48:1–12. <https://doi.org/10.1086/595011>.
3. Bouwknegt M, van Dorp S, Kuijper E. 2015. Burden of *Clostridium difficile* infection in the United States. *N Engl J Med* 372:2368. <https://doi.org/10.1056/NEJMc1505190#SA1>.

4. Rao GG. 1998. Risk factors for the spread of antibiotic-resistant bacteria. *Drugs* 55:323–330. <https://doi.org/10.2165/00003495-199855030-00001>.
5. Merianos JJ. 1991. Quaternary ammonium antimicrobial compounds, p 225–230. *In* Block SS (ed), *Disinfection, sterilization, and preservation*, 4th ed. Lea & Febiger, Philadelphia, PA.
6. Gilbert P, Moore LE. 2005. Cationic antiseptics: diversity of action under a common epithet. *J Appl Microbiol* 99:703–715. <https://doi.org/10.1111/j.1365-2672.2005.02664.x>.
7. Wessels S, Ingmer H. 2013. Modes of action of three disinfectant active substances: a review. *Regul Toxicol Pharmacol* 67:456–467. <https://doi.org/10.1016/j.yrtph.2013.09.006>.
8. Bore E, Hébraud M, Chafsey I, Chambon C, Skjaeret C, Moen B, Mørseth T, Langsrud Ø, Rudi K, Langsrud S. 2007. Adapted tolerance to benzalkonium chloride in *Escherichia coli* K-12 studied by transcriptome and proteome analyses. *Microbiology* 153:935–946. <https://doi.org/10.1099/mic.0.29288-0>.
9. Caldwell D, Cox WA, D'arcy PF, Rowe LR. 1961. The antibacterial activity of new derivatives of 4-aminoquinoline and 4-aminoquinaldine. *J Pharm Pharmacol* 13:554–564. <https://doi.org/10.1111/j.2042-7158.1961.tb11869.x>.
10. Daoud NN, Dickinson NA, Gilbert P. 1983. Antimicrobial activity and physico-chemical properties of some alkyldimethylbenzylammonium chlorides. *Microbios* 37:73–85.
11. Gilbert P, Al-Taae A. 1985. Antimicrobial activity of some alkyltrimethylammonium bromides. *Lett Appl Microbiol* 1:101–104. <https://doi.org/10.1111/j.1472-765X.1985.tb01498.x>.
12. Hugo WB, Frier M. 1969. Mode of action of the antibacterial compound dequalinium acetate. *Appl Microbiol* 17:118–127.
13. Inácio AS, Domingues NS, Nunes A, Martins PT, Moreno MJ, Estronca LM, Fernandes R, Moreno AJM, Borrego MJ, Gomes JP, Vaz WLC, Vieira OV. 2016. Quaternary ammonium surfactant structure determines selective toxicity towards bacteria: mechanisms of action and clinical implications in antibacterial prophylaxis. *J Antimicrob Chemother* 71:641–654. <https://doi.org/10.1093/jac/dkv405>.
14. Knox WE, Auerbach VH. 1949. The action of cationic detergents on bacteria and bacterial enzymes. *J Bacteriol* 58:443–452.
15. Moen B, Rudi K, Bore E, Langsrud S. 2012. Subminimal inhibitory concentrations of the disinfectant benzalkonium chloride select for a tolerant subpopulation of *Escherichia coli* with inheritable characteristics. *Int J Mol Sci* 13:4101–4123. <https://doi.org/10.3390/ijms13044101>.
16. Salton MRJ. 1951. The adsorption of cetyltrimethylammonium bromide by bacteria, its action in releasing cellular constituents and its bactericidal effects. *J Gen Microbiol* 5:391–404. <https://doi.org/10.1099/00221287-5-2-391>.
17. Yenson MM. 1947. Precipitating effect of cationic detergents on soluble starch. *Nature* 159:813. <https://doi.org/10.1038/159813a0>.
18. Araújo PA, Mergulhão F, Melo L, Simões M. 2014. The ability of an antimicrobial agent to penetrate a biofilm is not correlated with its killing or removal efficiency. *Biofouling* 30:675–683. <https://doi.org/10.1080/08927014.2014.904294>.
19. Klimek JW, Bailey JH. 1956. Factors influencing the rate of killing of *Escherichia coli* exposed to benzalkonium chloride. *Appl Microbiol* 4:53–59.
20. Russell AD. 2003. Biocide use and antibiotic resistance: the relevance of laboratory findings to clinical and environmental situations. *Lancet Infect Dis* 3:794–803. [https://doi.org/10.1016/S1473-3099\(03\)00833-8](https://doi.org/10.1016/S1473-3099(03)00833-8).
21. Tomlinson E, Brown MR, Davis SS. 1977. Effect of colloidal association on the measured activity of alkylbenzyltrimethylammonium chlorides against *Pseudomonas aeruginosa*. *J Med Chem* 20:1277–1282. <https://doi.org/10.1021/jm00220a010>.
22. Smith MG, Gianoulis TA, Pukatzki S, Mekalanos JJ, Ornston LN, Gerstein M, Snyder M. 2007. New insights into *Acinetobacter baumannii* pathogenesis revealed by high-density pyrosequencing and transposon mutagenesis. *Genes Dev* 21:601–614. <https://doi.org/10.1101/gad.1510307>.
23. Tucker AT, Nowicki EM, Boll JM, Knauf GA, Burdis NC, Trent MS, Davies BW. 2014. Defining gene-phenotype relationships in *Acinetobacter baumannii* through one-step chromosome gene inactivation. *mBio* 5:e01313-14. <https://doi.org/10.1128/mBio.01313-14>.
24. Boll JM, Crofts AA, Peters K, Cattoir V, Vollmer W, Davies BW, Trent MS. 2016. A penicillin-binding protein inhibits selection of colistin-resistant, lipooligosaccharide-deficient *Acinetobacter baumannii*. *Proc Natl Acad Sci U S A* 113:E6228–E6237. <https://doi.org/10.1073/pnas.1611594113>.
25. Henry R, Crane B, Powell D, Deveson Lucas D, Li Z, Aranda J, Harrison P, Nation RL, Adler B, Harper M, Boyce JD, Li J. 2015. The transcriptomic response of *Acinetobacter baumannii* to colistin and doripenem alone and in combination in an in vitro pharmacokinetics/pharmacodynamics model. *J Antimicrob Chemother* 70:1303–1313. <https://doi.org/10.1093/jac/dku536>.
26. Arroyo LA, Herrera CM, Fernandez L, Hankins JV, Trent MS, Hancock REW. 2011. The pmrCAB operon mediates polymyxin resistance in *Acinetobacter baumannii* ATCC 17978 and clinical isolates through phosphoethanolamine modification of lipid A. *Antimicrob Agents Chemother* 55:3743–3751. <https://doi.org/10.1128/AAC.00256-11>.
27. Vaara M. 1981. Increased outer membrane resistance to ethylenediaminetetraacetate and cations in novel lipid A mutants. *J Bacteriol* 148:426–434.
28. Sun J, Deng Z, Yan A. 2014. Bacterial multidrug efflux pumps: mechanisms, physiology and pharmacological exploitations. *Biochem Biophys Res Commun* 453:254–267. <https://doi.org/10.1016/j.bbrc.2014.05.090>.
29. Rajamohan G, Srinivasan VB, Gebreyes WA. 2010. Novel role of *Acinetobacter baumannii* RND efflux transporters in mediating decreased susceptibility to biocides. *J Antimicrob Chemother* 65:228–232. <https://doi.org/10.1093/jac/dkp427>.
30. Richmond GE, Evans LP, Anderson MJ, Wand ME, Bonney LC, Ivens A, Chua KL, Webber MA, Sutton JM, Peterson ML, Piddock LJV. 2016. The *Acinetobacter baumannii* two-component system AdeRS regulates genes required for multidrug efflux, biofilm formation, and virulence in a strain-specific manner. *mBio* 7:e00430-16. <https://doi.org/10.1128/mBio.00430-16>.
31. Yoon EJ, Chabane YN, Goussard S, Snesrud E, Courvalin P, Dé E, Grillot-Courvalin C. 2015. Contribution of resistance-modulation-cell division efflux systems to antibiotic resistance and biofilm formation in *Acinetobacter baumannii*. *mBio* 6:e00309-15. <https://doi.org/10.1128/mBio.00309-15>.
32. Kohanski MA, Dwyer DJ, Wierzbowski J, Cottarel G, Collins JJ. 2008. Mistranslation of membrane proteins and two-component system activation trigger antibiotic-mediated cell death. *Cell* 135:679–690. <https://doi.org/10.1016/j.cell.2008.09.038>.
33. Ling J, Cho C, Guo LT, Aerni HR, Rinehart J, Söll D. 2012. Protein aggregation caused by aminoglycoside action is prevented by a hydrogen peroxide scavenger. *Mol Cell* 48:713–722. <https://doi.org/10.1016/j.molcel.2012.10.001>.
34. Marr AK, Overhage J, Bains M, Hancock REW. 2007. The Lon protease of *Pseudomonas aeruginosa* is induced by aminoglycosides and is involved in biofilm formation and motility. *Microbiology* 153:474–482. <https://doi.org/10.1099/mic.0.2006/002519-0>.
35. Rosen R, Biran D, Gur E, Becher D, Hecker M, Ron EZ. 2002. Protein aggregation in *Escherichia coli*: role of proteases. *FEMS Microbiol Lett* 207:9–12. <https://doi.org/10.1111/j.1574-6968.2002.tb11020.x>.
36. Gur E, Biran D, Ron EZ. 2011. Regulated proteolysis in Gram-negative bacteria—how and when? *Nat Rev Microbiol* 9:839–848. <https://doi.org/10.1038/nrmicro2669>.
37. Tomoyasu T, Mogk A, Langen H, Goloubinoff P, Bukau B. 2001. Genetic dissection of the roles of chaperones and proteases in protein folding and degradation in the *Escherichia coli* cytosol. *Mol Microbiol* 40:397–413. <https://doi.org/10.1046/j.1365-2958.2001.02383.x>.
38. Frauenfeld J, Gumbart J, van der Sluis EO, Funes S, Gartmann M, Beatriz B, Mielke T, Berninghausen O, Becker T, Schulten K, Beckmann R. 2011. Cryo-EM structure of the ribosome-SecYE complex in the membrane environment. *Nat Struct Mol Biol* 18:614–621. <https://doi.org/10.1038/nsmb.2026>.
39. Robert F, Brakier-Gingras L. 2003. A functional interaction between ribosomal proteins S7 and S11 within the bacterial ribosome. *J Biol Chem* 278:44913–44920. <https://doi.org/10.1074/jbc.M306534200>.
40. Gomez JE, Kaufmann-Malaga BB, Wivagg CN, Kim PB, Silvius MR, Renedo N, Ioerger TR, Ahmad R, Livny J, Fishbein S, Sacchettini JC, Carr SA, Hung DT. 2017. Ribosomal mutations promote the evolution of antibiotic resistance in a multidrug environment. *Elife* 6:e20420. <https://doi.org/10.7554/eLife.20420>.
41. Perry M, de Groot MJ, Helliwell R, Leishman D, Tristani-Firouzi M, Sanguinetti MC, Mitcheson J. 2004. Structural determinants of HERG channel block by clofilium and ibutilide. *Mol Pharmacol* 66:240–249. <https://doi.org/10.1124/mol.104.000117>.
42. Rychter J, Espin F, Gallego D, Vergara P, Jiménez M, Clavé P. 2014. Colonic smooth muscle cells and colonic motility patterns as a target for irritable bowel syndrome therapy: mechanisms of action of otilonium bromide. *Ther Adv Gastroenterol* 7:156–166. <https://doi.org/10.1177/1756283X14525250>.
43. Tiku PE, Nowell PT. 1991. Selective inhibition of K(+) stimulation of

- Na,K-ATPase by bretylium. *Br J Pharmacol* 104:895–900. <https://doi.org/10.1111/j.1476-5381.1991.tb12523.x>.
44. Zhao YR, Ding L, Fan HW, Yu Y, Qi XM, Leng Y, Rao YK. 2010. Determination of the unstable drug otilonium bromide in human plasma by LC-ESI-MS and its application to a pharmacokinetic study. *J Chromatogr B Analyt Technol Biomed Life Sci* 878:2896–2900. <https://doi.org/10.1016/j.jchromb.2010.08.003>.
 45. Mah T-F. 2014. Establishing the minimal bactericidal concentration of an antimicrobial agent for planktonic cells (MBC-P) and biofilm cells (MBC-B). *J Vis Exp* (83):e50854. <https://doi.org/10.3791/50854>.
 46. Korman TM. 2015. Diagnosis and management of *Clostridium difficile* infection. *Semin Respir Crit Care Med* 36:31–43. <https://doi.org/10.1055/s-0034-1398741>.
 47. Tischer M, Pradel G, Ohlsen K, Holzgrabe U. 2012. Quaternary ammonium salts and their antimicrobial potential: targets or nonspecific interactions? *ChemMedChem* 7:22–31. <https://doi.org/10.1002/cmdc.201100404>.
 48. Hashimoto T, Maruoka K. 2007. Recent development and application of chiral phase-transfer catalysts. *Chem Rev* 107:5656–5682. <https://doi.org/10.1021/cr068368n>.
 49. Maillard JY. 2007. Bacterial resistance to biocides in the healthcare environment: should it be of genuine concern? *J Hosp Infect* 65(Suppl 2):60–72. [https://doi.org/10.1016/S0195-6701\(07\)60018-8](https://doi.org/10.1016/S0195-6701(07)60018-8).
 50. Kramer G, Rauch T, Rist W, Vorderwülbecke S, Patzelt H, Schulze-Specking A, Ban N, Deuerling E, Bukau B. 2002. L23 protein functions as a chaperone docking site on the ribosome. *Nature* 419:171–174. <https://doi.org/10.1038/nature01047>.
 51. Nowotny V, Nierhaus KH. 1982. Initiator proteins for the assembly of the 50S subunit from *Escherichia coli* ribosomes. *Proc Natl Acad Sci U S A* 79:7238–7242.
 52. Bousquet E, Cecchetti V, De Regis M, Mannucci E, Orzalesi G, Volpato I. 1984. Quaternary salts of aminoethyl-p-aminobenzoates and aminoethyl-p-aminobenzamides. Synthesis and pharmacologic activity. *Farm Ed Sci* 39:3–15.
 53. Triantafyllidis JK, Malgarinos G. 2014. Long-term efficacy and safety of otilonium bromide in the management of irritable bowel syndrome: a literature review. *Clin Exp Gastroenterol* 7:75–82. <https://doi.org/10.2147/CEG.S46291>.
 54. Bhattarai Y, Muniz Pedrogo DA, Kashyap PC. 2017. Irritable bowel syndrome: a gut microbiota-related disorder? *Am J Physiol Gastrointest Liver Physiol* 312:G52–G62. <https://doi.org/10.1152/ajpgi.00338.2016>.
 55. McMurry LM, Oethinger M, Levy SB. 1998. Triclosan targets lipid synthesis. *Nature* 394:531–532. <https://doi.org/10.1038/28970>.
 56. Lu H, Tonge PJ. 2008. Inhibitors of FabI, an enzyme drug target in the bacterial fatty acid biosynthesis pathway. *Acc Chem Res* 41:11–20. <https://doi.org/10.1021/ar700156e>.
 57. Wiegand I, Hilpert K, Hancock REW. 2008. Agar and broth dilution methods to determine the minimal inhibitory concentration (MIC) of antimicrobial substances. *Nat Protoc* 3:163–175. <https://doi.org/10.1038/nprot.2007.521>.
 58. Dong TG, Ho BT, Yoder-Himes DR, Mekalanos JJ. 2013. Identification of T6SS-dependent effector and immunity proteins by Tn-seq in *Vibrio cholerae*. *Proc Natl Acad Sci U S A* 110:2623–2628. <https://doi.org/10.1073/pnas.1222783110>.
 59. Davies BW, Bogard RW, Young TS, Mekalanos JJ. 2012. Coordinated regulation of accessory genetic elements produces cyclic di-nucleotides for *V. cholerae* virulence. *Cell* 149:358–370. <https://doi.org/10.1016/j.cell.2012.01.053>.
 60. Wang N, Ozer EA, Mandel MJ, Hauser AR. 2014. Genome-wide identification of *Acinetobacter baumannii* genes necessary for persistence in the lung. *mBio* 5:e01163-14. <https://doi.org/10.1128/mBio.01163-14>.
 61. Li Q, Lex RK, Chung H, Giovanetti SM, Ji Z, Ji H, Person MD, Kim J, Vokes SA. 2016. The pluripotency factor NANOG binds to GLI proteins and represses hedgehog-mediated transcription. *J Biol Chem* 291:7171–7182. <https://doi.org/10.1074/jbc.M116.714857>.
 62. Keller A, Nesvizhskii AI, Kolker E, Aebersold R. 2002. Empirical statistical model to estimate the accuracy of peptide identifications made by MS/MS and database search. *Anal Chem* 74:5383–5392. <https://doi.org/10.1021/ac025747h>.
 63. Nesvizhskii AI, Keller A, Kolker E, Aebersold R. 2003. A statistical model for identifying proteins by tandem mass spectrometry. *Anal Chem* 75:4646–4658. <https://doi.org/10.1021/ac0341261>.
 64. Ashburner M, Ball CA, Blake JA, Botstein D, Butler H, Cherry JM, Davis AP, Dolinski K, Dwight SS, Eppig JT, Harris MA, Hill DP, Issel-Tarver L, Kasarskis A, Lewis S, Matese JC, Richardson JE, Ringwald M, Rubin GM, Sherlock G. 2000. Gene ontology: tool for the unification of biology. The Gene Ontology Consortium. *Nat Genet* 25:25–29. <https://doi.org/10.1038/75556>.
 65. Jacobs AC, Thompson MG, Black CC, Kessler JL, Clark LP, McQueary CN, Gancz HY, Corey BW, Moon JK, Si Y, Owen MT, Hallock JD, Kwak YI, Summers A, Li CZ, Rasko DA, Penwell WF, Honnold CL, Wise MC, Waterman PE, Lesho EP, Stewart RL, Actis LA, Palys TJ, Craft DW, Zurawski DV. 2014. AB5075, a highly virulent isolate of *Acinetobacter baumannii*, as a model strain for the evaluation of pathogenesis and antimicrobial treatments. *mBio* 5:e01076-14. <https://doi.org/10.1128/mBio.01076-14>.
 66. Zhang SK, Song JW, Gong F, Li SB, Chang HY, Xie HM, Gao HW, Tan YX, Ji SP. 2016. Design of an α -helical antimicrobial peptide with improved cell-selective and potent anti-biofilm activity. *Sci Rep* 6:27394. <https://doi.org/10.1038/srep27394>.